

Gravity is not a Pairwise Local Classical Channel

Natacha Altamirano,^{1,2,*} Paulina Corona-Ugalde,^{3,2,†} Robert B. Mann,^{1,3,2,‡} and Magdalena Zych^{4,§}

¹*Perimeter Institute for Theoretical Physics, 31 Caroline St. N. Waterloo Ontario, N2L 2Y5, Canada*

²*Department of Physics and Astronomy, University of Waterloo, Waterloo, Ontario, Canada, N2L 3G1*

³*Institute for Quantum Computing, University of Waterloo, Waterloo, Ontario, N2L 3G1, Canada*

⁴*Centre for Engineered Quantum Systems, School of Mathematics and Physics,
The University of Queensland, St Lucia, Queensland 4072, Australia*

(Dated: March 1, 2022)

It is currently believed that there is no experimental evidence on possibly quantum features of gravity or gravity-motivated modifications of quantum mechanics. Here we show that single-atom interference experiments achieving large spatial superpositions can rule out a framework where the Newtonian gravitational interaction is fundamentally classical in the information-theoretic sense: it cannot convey entanglement. Specifically, in this framework gravity acts pairwise between massive particles as classical channels, which effectively induce approximately Newtonian forces between the masses. The experiments indicate that if gravity does reduce to the pairwise Newtonian interaction between atoms at the low energies, this interaction cannot arise from the exchange of just classical information, and in principle has the capacity to create entanglement. We clarify that, contrary to current belief, the classical-channel description of gravity differs from the model of Diosi and Penrose, which is not constrained by the same data.

There is an overwhelming experimental evidence that properties of local physical systems are incompatible with a fully local classical description [1–8]. Nevertheless, the possibility that gravity remains classical at a fundamental level is considered viable or even necessary [9–18], with a range of arguments invoked to support such a position: absence of direct observations of quantum gravitational phenomena [19], anticipated pernicious tensions between the foundational principles of quantum theory and general relativity [16, 17, 20] (see e.g. [21, 22] for different views), and lack of a complete framework for quantum gravity [23].

From an information-theoretic perspective, classicality of an interaction is defined as the inability of the resulting channel to increase entanglement. Thus, in order to verify whether gravity is a quantum or a classical entity it has been proposed to test its entangling capacity using a pair of masses in two close-by interferometers [24–26].

Here we take a different approach and explore consequences of the assumption that gravity is fundamentally classical in the information-theoretic sense, and is incapable of creating entanglement. Since a unitary interaction in general does increase entanglement, an interaction with a known unitary part must be accompanied by decoherence in order for the resulting channel to be entanglement non-increasing – a model-independent result shows that this decoherence must be at least twice the interaction strength [27, 28] (see also [29, 30] for a broader context of effective dynamics in a classical stochastic environment).

The presence of the unitary Newtonian term in the Schrödinger equation is experimentally well established [31–35]. Therefore, for gravity to be a fundamentally classical channel the unitary Newtonian term must be accompanied by

certain minimal decoherence – first shown in a series of works by Kafri, Taylor and Milburn (KTM) [27, 36, 37]. The significance of the KTM approach is that it provides a broad framework for understanding how to describe gravitational interactions in an information-theoretic manner, and their lower bound on decoherence distinguishes theories where low-energy particles can or cannot develop entanglement through the Newtonian interaction.

Here we show that this information-theoretic notion of classicality of gravity is incompatible with the results of recent atom interference experiments [38, 39], heavily constraining the possibility that gravity acts as pairwise classical channels effectively inducing Newtonian force at low energies. While current experiments do not directly prove that gravity does entangle massive particles, they nevertheless constrain the same model that would be tested in experiments proposed in refs [24–26]. Furthermore, we show that decoherence resulting from the KTM approach is conceptually and quantitatively different from decoherence in the Diosi-Penrose (DP) and related models [13–16, 40], not refuted by the same data.

I. EFFECTIVE GRAVITY FROM LOCAL, CLASSICAL CHANNELS

The KTM framework is an application of pairwise continuous measurement with feedback [29, 30] to gravitational interactions. It can also be obtained from a quantum collisional model, where the systems interact with a Markovian environment in a suitably chosen parameter regime [28]. Below we summarize key aspects of this approach [36] (see also Appendix A).

Consider a pair of particles interacting with a set of ancillae (environment). The assumptions are: a) particles interact with the ancillae but not with each other; b) the interactions are local and any information transmitted through the ancillae is classical c) the unitary part of the channel reduces to the standard Newtonian pair-potential at low energies. The ancilla can

* naltamirano@perimeterinstitute.ca

† pcoronau@uwaterloo.ca

‡ rbmann@uwaterloo.ca

§ m.zych@uq.edu.au

here be regarded as gravitational degrees of freedom and they facilitate measurement-and-feedback scenario, equivalent to averaging over definite but unknown measurement outcomes and correspondingly applied local feedback. The framework thus defines a Local Operations and Classical Communication (LOCC) channel [41] between the pair of masses. The resulting dynamics of two particles along the radial, x , direction is obtained by tracing over the ancilla and reads

$$\dot{\rho}_{12} = -\frac{i}{\hbar}[\hat{H}_0 + V_0, \rho_{12}] - \left(\frac{1}{4D} + \frac{K^2 D}{4\hbar^2}\right) \sum_{i=1}^2 [\hat{x}_i, [\hat{x}_i, \rho_{12}]], \quad (1)$$

where ρ_{12} is the state of both particles and \hat{x}_1, \hat{x}_2 is the displacement from the initial position of the respective particle. The effective unitary interaction $V_0 = K\hat{x}_1\hat{x}_2 +$ (local terms in \hat{x}_1, \hat{x}_2), for $K := 2\frac{Gm_1m_2}{d^3}$ approximates the Newtonian potential between masses m_1, m_2 at a distance $d + x_1 + x_2$; i.e. $V_0 \approx -G\frac{m_1m_2}{[d+x_1+x_2]}$ up to second order in $x_i, i = 1, 2$. It is accompanied by non-unitary terms, given by the double commutators, describing decoherence in the position basis: For each particle, the magnitude of its off-diagonal elements x_i, x'_i decays at a rate $\Gamma_{\text{KTM}} = \left(\frac{1}{4D} + \frac{K^2 D}{4\hbar^2}\right) \Delta x^2$, where $\Delta x = |x_i - x'_i|$ is the “superposition size” of the i -th particle. Importantly, Γ_{KTM} has a non-vanishing lower bound $\propto \frac{K}{2\hbar}$. The decoherence rate of each particle is thus fully characterised by the gradient of the Newtonian force between the masses, $\frac{K}{2} = \frac{Gm_1m_2}{d^3}$, and by the superposition size Δx :

$$\Gamma_{\text{KTM}}^{\min} = \frac{K}{2\hbar} \Delta x^2. \quad (2)$$

The effective interaction is necessarily accompanied by decoherence of at least the same strength since LOCC channels are entanglement non-increasing [41] (see also ref. [28] for a discussion in this specific context). If the decoherence rate is smaller than $\Gamma_{\text{KTM}}^{\min}$, the unitary term V_0 can increase entanglement between the particles [36] – this is independent of the specific model for the channel or the ancilla. Any dynamical theory of gravity giving rise to the same unitary term as in eq. (1) but with smaller decoherence, can in principle generate entanglement and is therefore not fundamentally classical, (not compatible with an LOCC channel).

A. Composite systems

We shall apply the KTM approach to a pair of systems comprising an atom in an interferometer and the Earth. We first demonstrate that upon extending the KTM model to macroscopic systems the lower bound on decoherence (2) remains unchanged up to a factor related to the geometry of the bodies (see Appendix B).

Let s_1, s_2 be rigid bodies with total masses M_1, M_2 , comprising N_1, N_2 elementary constituents, respectively, with masses $m_i, i = 1, \dots, N_1 + N_2$. We take the minimum of the decoherence rates, as in eq. (2), for each pair, whose evolution is described by eq. (1). We consider s_1 to be a test mass, in a superposition of different radial distances from the body

s_2 which describes all the remaining matter (Earth, ~ 500 kg of tungsten [33], etc) and is thus considered initially well localised. The resulting dynamics of the centre-of-mass (CM) of s_1 , in the radial direction, is described by

$$\dot{\rho}_{s_1} = -\frac{i}{\hbar}[\hat{H}_0 + V, \rho_{s_1}] - \mathcal{D}_{\min}[\hat{r}_1, [\hat{r}_1, \rho_{s_1}]], \quad (3)$$

where $V \approx -G\frac{M_1M_2}{[d+r_1+r_2]}$, with r_k the displacement of the CM of s_k and

$$\mathcal{D}_{\min} := \frac{1}{2\hbar} \left(\sum_{i \neq j \in s_1} |K_{ij}| + \sum_{i \in s_1} \sum_{j \in s_2} |K_{ij}| \right), \quad (4)$$

where K_{ij} is the Newtonian force gradient between the masses m_i, m_j in three dimensions. The non-unitary term is simply the sum of pairwise contributions from all constituents of the bodies. The corresponding minimal decoherence rate reads

$$\tilde{\Gamma}_{\text{KTM}}^{\min} = \mathcal{D}_{\min} \Delta x^2. \quad (5)$$

The sum of the unitary contributions approximates Newtonian interactions between all constituents – which is the gravitational potential energy between two point masses M_1, M_2 . However, the decoherence rate (4) in general differs from that for two elementary masses: first, it contains terms connecting constituents of s_1 (first sum), and s_1 with s_2 (second sum). Second, for non-convex bodies the rate (5) might be smaller than the rate given by the original model, eq. (2) applied to the CMs of s_1, s_2 (e.g. when s_2 is a spherical shell of matter with s_1 at the centre). For an elementary test mass m near the surface of a homogeneous ball of mass M and radius R , the KTM decoherence rate is at least as large as (see Appendix B)

$$\Gamma_{\text{KTM}}^{\min} \geq \tilde{\Gamma}_{\text{KTM}}^C = C \frac{GMm}{\hbar R^3} \Delta x^2, \quad (6)$$

with $C \simeq 0.47$ for this particular geometry. For $C = 1$ the above reduces to the original KTM model applied directly to the CMs of the two systems.

Note that in general one cannot here approximate the mass distributions to be continuous, since contributions from the body’s own constituents diverge and an explicit definition of the *fundamental* constituents is needed. We propose that these should be the smallest constituents between which the binding energy contribution to the total mass can be neglected (since the total mass of the system is here the sum of the masses of its constituents). We hereafter consider atoms as such fundamental constituents.

II. KTM VS ATOMIC FOUNTAINS

We can now confront the KTM proposal against two interferometric tests with atoms that use large momentum transfer (LMT) [38, 39]. We treat the interfering atom as a test mass s_1 and Earth as the massive ball s_2 in eq. (6).

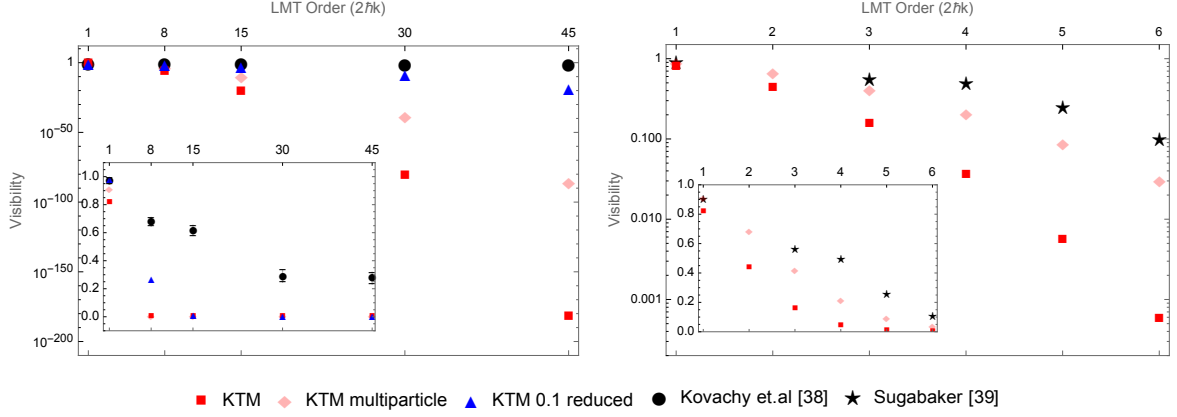


FIG. 1. Logarithm of the interferometric visibility as a function of the superposition size (LMT order) reported in ref. [38] (black dots, left panel – including the reported error bars) and in ref. [39] (black stars, right panel) vs the prediction of the KTM model eq. (7) for $C = 1$ (red squares), its multi particle correction $C = 0.47$ (pink diamonds), reduced KTM correction $C = 0.1$ (blue triangles). (The insets represent the same data in a linear scale.) Both experiments used ^{87}Rb ; the reported superpositions were up to 8.2 cm in [39] and 54cm in [38]. Both experiments contravene the KTM model (including its multi-particle formulation).

In LMT interferometers a sequence of $N \frac{\pi}{2}$ laser pulses implements a beam splitter, preparing the atoms in a superposition of wave packets with momentum difference $2N\hbar k$ in the vertical direction, where k is the laser wave-number. For time T the wave packets propagate freely and thus spatially separate; then a sequence of π -pulses exchanges their momenta and at time $2T$ the wave packets interfere at a final beam splitter ($N \frac{\pi}{2}$ -pulses). For an atom of mass m the vertical separation between the wave packets is $\Delta x(t) = 2N\hbar k t/m$ for $t < T$, it then symmetrically decreases until $t = 2T$. Eq. (3) entails that the magnitude of the off-diagonal elements of the atom $V(t) := |\langle r_1 | \rho_{s_1} | r_2 \rangle(t)|$ at the end of the interferometric sequence reads $V(2T) = |\langle r_1 | \rho_{s_1} | r_2 \rangle(0)| e^{-\int_0^{2T} dt \mathcal{D}_{min} \Delta x^2(t)}$. Since $V(2T)$ describes the visibility of the interference pattern attainable in the experiment, the maximal visibility allowed by the classical channel framework for atom fountains on Earth is estimated as $e^{-2 \int_0^T dt \tilde{\Gamma}_{KTM}^C}$, which for the above $\Delta x(t)$ reads:

$$V_{KTM}^{max} = e^{-\frac{2}{3} C \frac{G \hbar M_{\oplus}}{m R_{\oplus}^3} (2Nk)^2 T^3}. \quad (7)$$

In Fig. 1 we compare this prediction for $C = 1$ (the original KTM model), $C = 0.47$ (our multi particle correction), and $C = 0.1$ (arbitrary down-scaling of the decoherence rate) against measured visibilities [38] and [39] (noting at this point the controversy [42] regarding ref. [38]). The values of the relevant parameters are $M_{\oplus} = 6 \cdot 10^{24}$ kg; $R_{\oplus} = 6 \cdot 10^3$ km, $\frac{\hbar k}{m} = 5.8 \frac{\text{mm}}{\text{s}}$, $m = 1.4 \cdot 10^{-25}$ kg (^{87}Rb); $T = 1.15$ s in Ref. [39] and $T = 1.04$ s in Ref. [38].

Both the original KTM model ($C = 1$) and the multi particle correction ($C = 0.47$) predict maximal visibilities that are well below the measured ones. Taking into account finite duration of light-atom interactions would introduce a correction to the path separation. In the insets of Fig. 1 we show that even if this resulted in a reduction of the decoherence rate to $C = 0.1$, the resulting visibilities would still be smaller than the measured ones by factors ranging from ~ 2.5 to $\sim 10^{18}$.

III. COMPARISON TO THE DIOSI-PENROSE MODEL

The experiments refuting the classical-channel description of gravity do not constrain the DP model; see Table I. As the KTM approach and the DP model are thought to give equivalent decoherence rates [15, 36], we discuss below their key differences. In the DP model decoherence is quantified by a “self-interaction” between the superposed amplitudes of a system: for a rigid body (and in particular for an elementary mass) $\Gamma_{DP} = \frac{1}{2\hbar} [U(XX) + U(YY) - 2U(XY)]$, where $U(XY) = -G \int d^3r \int d^3r' \frac{f_X(r)f_Y(r')}{|r-r'|}$ is a gravitational energy between two mass-distributions f_X, f_Y which are here associated with two superposed configurations X, Y of the same system [14]. By contrast, in the KTM approach decoherence depends on the gravitational interaction between *different* systems. As a result, both frameworks predict decoherence in the position basis, whose magnitude is related to gravity, but differ both quantitatively (Table I) and conceptually (Table II) as follows:

a. For a point particle Γ_{DP} diverges and requires a cut-off δ in the *coherent spread* of the particle’s wave-function [14], whereas the KTM approach is well-defined for point particles.

b. A single elementary particle in an otherwise empty universe decoheres in the DP model, but does not decohere in the KTM approach: if other systems are removed far from the particle $\tilde{\Gamma}_{KTM}^{min} \rightarrow 0$, Table II row (i). This is an important feature since for a single particle in an otherwise empty universe the notion of “location” has no physical meaning. Thus, arguing that the particle is – or is not – in a superposition of “two different locations” has no physical meaning either – and the scenario cannot give rise to any physical effect.

c. KTM decoherence crucially depends on the distance d between the test particle and other masses: For fixed M and Δx : $0 < \Gamma_{KTM}^{min} < \frac{mc^2}{\hbar} (\frac{\Delta x}{R_S})^2$ where the lower bound

TABLE I. Comparison of decoherence times $1/\Gamma_{\text{DP}}$ and $1/\Gamma_{\text{KTM}}^{\text{min}}$ predicted by DP and KTM models for matter-wave interference experiments [33, 38, 43, 44]. For all tests $1/\Gamma_{\text{KTM}}^{\text{min}}$ contains the contribution from Earth $M_{\oplus} \sim 6 \times 10^{24}$ kg, $R_{\oplus} \sim 6 \times 10^3$ km, and for experiment [33] additionally from 24 bars of tungsten^a each with mass ~ 21.5 kg, and 6 of each at approximate distances of 107.6 mm, 177.6 mm, 279.5 mm and 313.1 mm from the atoms. For Γ_{DP} we took $\delta = 10^{-15}$. Labels deonte: m – mass of the interfering particles; M – “source” mass/masses; d – distance between the source and the test mass (both relevant only for Γ_{KTM}); Δx – superposition size. For simplicity we treat all test masses as single particles.

Experiment	m [Kg]	M [Kg]	d [m]	Δx [m]	$1/\Gamma_{\text{DP}}$ [s]	$1/\Gamma_{\text{KTM}}^{\text{min}}$ [s]
10 m atomic fountain with ^{87}Rb [38]	1.4×10^{-25}	M_{\oplus}	R_{\oplus}	0.54	3×10^{10}	2×10^{-3}
two atomic fountains with ^{87}Rb [33] (operating as gravity-gradiometer)	1.4×10^{-25}	M_{\oplus} 4×129	R_{\oplus} 0.11, 0.18, 0.28, 0.31	1.86×10^{-3}	3×10^{10}	2×10^1
large-molecule interferometry [43]	1.6×10^{-23}	M_{\oplus}	R_{\oplus}	2.7×10^{-7}	3×10^6	6×10^7
PcH ₂ diffraction on alga skeleton [44]	8.2×10^{-25}	M_{\oplus}	R_{\oplus}	2×10^{-7}	1×10^9	2×10^9

^a Tungsten bars were used to induce controllable gravity gradient between two atom interferometers operating as gravity gradiometer.

TABLE II. General form of the decoherence rates Γ_{DP} (Diosi-Penrose) and $\tilde{\Gamma}_{\text{KTM}}^{\text{min}}$ (Kafri-Taylor-Milburn) (5) for spherical mass distributions [14, 45]. δ denotes the cut-off of the DP model, and Δx is the superposition size. Case (iii) considers decoherence of the CM of a body comprising N_1 constituents of mass m in the presence of another body comprising N_2 masses m . Whereas $\tilde{\Gamma}_{\text{KTM}}^{\text{min}}$ depends on the gravitational force gradients between *different* particles, Γ_{DP} depends on the *self-interaction* between superposed amplitudes of the same particle.

Scenario:	Γ_{DP}	$\tilde{\Gamma}_{\text{KTM}}^{\text{min}}$
(i) single particle mass m	$\frac{Gm^2\Delta x^2}{2\delta^3\hbar}$ for $\delta \gg \Delta x$ $\frac{2Gm^2}{\delta\hbar} \left(\frac{6}{5} - \frac{\delta}{\Delta x} \right)$ for $\delta \ll \Delta x$	0
(ii) two particles masses m, M ; distance d	same as (i)	$\frac{GmM\Delta x^2}{d^3\hbar} = \begin{cases} 0, & d \rightarrow \infty \\ \frac{mc^2}{\hbar} \left(\frac{\Delta x}{R_S} \right)^2, & d \rightarrow R_S := \frac{2GM}{c^2} \end{cases}$
(iii) two composite bodies; masses $N_1 m, N_2 m$; dist. d_{ij}	$N_1 \frac{Gm^2\Delta x^2}{2\delta^3\hbar}$; $\delta \gg \Delta x$ $N_1 \frac{2Gm^2}{\delta\hbar} \left(\frac{6}{5} - \frac{\delta}{\Delta x} \right)$ for $\delta \ll \Delta x$	$\frac{\Delta x^2}{2\hbar} \left(\sum_{i \neq j=1}^{N_1} K_{ij} + \sum_{i=1}^{N_1} \sum_{j=N_1+1}^{N_1+N_2} K_{ij} \right)$

holds for $d \rightarrow \infty$ and the upper for $d = R_S = 2GM/c^2$ (the Schwarzschild radius of M), Table II row (ii). In contrast, Γ_{DP} for a single particle is independent of its gravitational environment.

d. The KTM “self interaction” terms – first sum in eq. (4), Table II row (iii) – are purely classical: They connect *different constituents* of a composite system, not different points of a single system wave-function.

e. The KTM proposal predicts vanishing decoherence when all force gradients K_{ij} are negligible, i.e. the sum of the homogeneous field contributions is induced without decoherence. It is thus compatible (to a limited extent) with the equivalence principle, as it does not predict any decoherence in the above case as well as for an accelerating particle.

IV. DISCUSSION

We have shown that an LOCC gravity framework is very strongly constrained by experiments. Our analysis relies on certain auxiliary assumptions, particularly regarding the mass distribution of the earth and that all N laser pulses comprising each π and $\pi/2$ atom-light interaction are applied effectively simultaneously. While these assumptions do not seem to pose

a formidable challenge to our conclusions, one certainly can improve on the presented analysis: one example is to use an atom-fountain gravity-gradiometer (two interferometers with vertical separation L) and a large mass M (in the plane of, say, the lower interferometer), whose horizontal distance d_h to the atoms can be varied [33–35], cf. Table I. A continuous mode of operation could be considered for improved sensitivity [46]. The KTM proposal predicts a different phase noise in the two interferometers as a function of d_h . With $M = 252$ kg and $0.25 < d_h < 0.5$ m, an experiment at LMT order $10\hbar k$ and $T = 0.5$ s would see the lower interferometer’s contrast varying between 0.5–0.65, while the upper – between 0.62–0.64.

Thus far, tests of the KTM framework were suggested with optomechanical or torsion balance setups. However, even including Earth into the analysis, as in the present work, such tests would face a formidable challenge. For an optomechanical experiment, in order to detect KTM decoherence on top of the thermal noise, the mechanical frequency Ω , quality factor Q and the temperature T of the mechanical oscillator must satisfy $T\Omega/Q < G\hbar M_{\oplus}/2k_B R_{\oplus}^3 \sim 10^{-18}$ K/s, where k_B is the Boltzmann constant; a state of the art setup [47] with $Q = 2 \times 10^7$, $\Omega/2\pi = 1$ Hz, $T = 4$ K yields $T\Omega/Q \sim 10^{-6}$ K/s. For the original KTM model to be discernible from mea-

surement noise, the measurement frequency ω must satisfy $\omega^2 < GM_{\oplus}/R_{\oplus}^3 \sim 10^{-6} \text{ Hz}^2$, whereas the value considered in [47] (at the standard quantum limit) gives $\omega^2 \sim 10^6 \text{ Hz}^2$. Current optomechanical sensitivities would thus still need to be improved in order to test KTM assumptions. For torsion balance setups with 1–10 kg masses KTM approach yields $\Gamma_{\text{KTM}}^{\text{min}} \sim 10^{25} \text{ Hz}$, while experimental bound obtained from refs [48, 49], is $\sim 10^{40} \text{ Hz}$ (see Appendix C).

From the theoretical-physics perspective, an immediate question is how much entanglement (what channel capacity) suffices to reproduce the experimental results? In order to address this question, it would be desirable to formulate an extension of the KTM approach – describing gravitational interactions beyond the Newtonian limit, as well as allowing for larger channel capacities. (Any “complete” framework that has Newtonian gravity as its low-energy limit cannot be mediated by DOFs which are fundamentally classical and interact with the constituents of massive bodies in a local fashion – as this would require the Newtonian limit of such a framework to be compatible with an LOCC channel, which contradicts experiments.) We note here that three models exploring various aspects of the KTM approach in different relativistic contexts have already been put forward [50–52] and frameworks with an increased channel capacity, can be constructed e.g. by relaxing the assumption of local system-ancilla interactions or constraining the amount of energy introduced to the system by the ancilla [51]. Empirically constraining such models and understanding their ramifications for the gravitationally induced entanglement remains an interesting subject for further investigation.

V. CONCLUSION

Results of the recent atom interference experiments very strongly constrain the worldview in which gravity reduces to the Newtonian pair potential at low energies *and* is also fundamentally classical: mediated by LOCC channels acting pairwise between atoms. We have further shown that – contrary to current belief – the KTM framework is not equivalent to the DP model. It is noteworthy that the same experiments do not constrain also other alternative models (gravity-

related or not) including continuous spontaneous localisation, or Schrödinger-Newton theory [40, 53, 54]. This raises a question about the notion of classicality of gravity in the DP and other models, and about their information-theoretic aspects. It is considered that such models allow for gravity to remain classical, but in the light of our analysis such claims need to be clarified: if the gravitational DOFs are to remain classical and yield Newtonian gravity at low-energies, some non-locality in their interactions with the masses needs to be allowed. An example of the latter case is semi-classical gravity, where the gravitational DOFs interact with the mean position of the source mass [23].

The understanding of the classical vs quantum properties of gravity is far from clear [55] and needs further work. However, the fact that the KTM framework can be empirically tested opens a novel route of investigation, one that focuses on a robust information-theoretic characterization of channels implied by alternative approaches to quantizing (or not quantizing) gravity. From a broader perspective, our work demonstrates that general frameworks as well as specific models for gravitational decoherence previously thought to be out of reach can be experimentally tested.

VI. ACKNOWLEDGMENTS

The authors thank S. Basiri Esfahani, W. Bowen, F. Costa, L. Diosi, S. Forstner, K. Khosla, G. Milburn, and A. Tilloy for discussions. This work was supported in part by the Natural Sciences and Engineering Research Council of Canada, ARC Centre of Excellence for Engineered Quantum Systems grant no. CE110001013 and the University of Queensland through UQ Fellowships grant no. 2016000089. Research at Perimeter Institute is supported by the Government of Canada through Industry Canada, by the Province of Ontario through the Ministry of Research and Innovation. P.C-U. gratefully acknowledges funding from CONACYT. N.A., P.C-U. and R.B.M are grateful for the hospitality of the University of Queensland where this work was initiated. M.Z. acknowledges the traditional owners of the land on which the University of Queensland is situated, the Turrbal and Jagera people.

-
- [1] A. Aspect, P. Grangier, and G. Roger, “Experimental Tests of Realistic Local Theories via Bell’s Theorem,” *Phys. Rev. Lett.* **47**, 460–463 (1981).
 - [2] M. Giustina, A. Mech, S. Ramelow, B. Wittmann, J. Kofler, J. Beyer, A. Lita, B. Calkins, T. Gerrits, S. W. Nam, R. Ursin, and A. Zeilinger, “Bell violation using entangled photons without the fair-sampling assumption,” *Nature* **497**, 227–230 (2013).
 - [3] B. Hensen, H. Bernien, A. E. Dréau, A. Reiserer, N. Kalb, M. S. Blok, J. Ruitenbergh, R. F. L. Vermeulen, R. N. Schouten, C. Abellán, W. Amaya, V. Pruneri, M. W. Mitchell, M. Markham, D. J. Twitchen, D. Elkouss, S. Wehner, T. H. Taminiau, and R. Hanson, “Loophole-free Bell inequality violation using electron spins separated by 1.3 kilometres,” *Nature (London)* **526**, 682–686 (2015).
 - [4] M. Giustina, M. A. M. Versteegh, S. Wengerowsky, J. Handsteiner, A. Hochrainer, K. Phelan, F. Steinlechner, J. Kofler, J.-A. Larsson, C. Abellán, W. Amaya, V. Pruneri, M. W. Mitchell, J. Beyer, T. Gerrits, A. E. Lita, L. K. Shalm, S. W. Nam, T. Scheidl, R. Ursin, B. Wittmann, and A. Zeilinger, “Significant-Loophole-Free Test of Bell’s Theorem with Entangled Photons,” *Phys. Rev. Lett.* **115**, 250401 (2015).
 - [5] L. K. Shalm, E. Meyer-Scott, B. G. Christensen, P. Bierhorst, M. A. Wayne, M. J. Stevens, T. Gerrits, S. Glancy, D. R. Hamel, M. S. Allman, K. J. Coakley, S. D. Dyer, C. Hodge,

- A. E. Lita, V. B. Verma, C. Lambrocco, E. Tortorici, A. L. Migdall, Y. Zhang, D. R. Kumor, W. H. Farr, F. Marsili, M. D. Shaw, J. A. Stern, C. Abellán, W. Amaya, V. Pruneri, T. Jennewein, M. W. Mitchell, P. G. Kwiat, J. C. Bienfang, R. P. Mirin, E. Knill, and S. W. Nam, “Strong Loophole-Free Test of Local Realism*,” *Phys. Rev. Lett.* **115**, 250402 (2015).
- [6] G. Kirchmair, F. Zähringer, R. Gerritsma, M. Kleinmann, O. Gühne, A. Cabello, R. Blatt, and C. F. Roos, “State-independent experimental test of quantum contextuality,” *Nature* **460**, 494–497 (2009).
- [7] R. Lapkiewicz, P. Li, C. Schaeff, N. K. Langford, S. Ramelow, M. Wieśniak, and A. Zeilinger, “Experimental non-classicality of an indivisible quantum system,” *Nature* **474**, 490–493 (2011).
- [8] X.-M. Hu, J.-S. Chen, B.-H. Liu, Y. Guo, Y.-F. Huang, Z.-Q. Zhou, Y.-J. Han, C.-F. Li, and G.-C. Guo, “Experimental Test of Compatibility-Loophole-Free Contextuality with Spatially Separated Entangled Qutrits,” *Physical Review Letters* **117**, 170403 (2016).
- [9] F. Karolyhazy, “Gravitation and quantum mechanics of macroscopic objects,” *Il Nuovo Cimento A* **42**, 390–402 (1966).
- [10] M. J. Hall and M. Reginatto, “Interacting classical and quantum ensembles,” *Physical Review A* **72**, 062109 (2005).
- [11] M. Albers, C. Kiefer, and M. Reginatto, “Measurement analysis and quantum gravity,” *Phys. Rev. D* **78**, 064051 (2008).
- [12] M. J. Hall and M. Reginatto, *Ensembles on Configuration Space: Classical, Quantum, and Beyond*, vol. 184. Springer, 2016.
- [13] L. Diosi, “Models for universal reduction of macroscopic quantum fluctuations,” *Physical Review A* **40**, 1165 (1989).
- [14] L. Diosi, “Notes on certain Newton gravity mechanisms of wavefunction localization and decoherence,” *Journal of Physics A: Mathematical and Theoretical* **40**, 2989 (2007).
- [15] A. Tilloy and L. Diosi, “Sourcing semiclassical gravity from spontaneously localized quantum matter,” *Phys. Rev. D* **D93**, 024026 (2016).
- [16] R. Penrose, “On gravity’s role in quantum state reduction,” *General Relativity and Gravitation* **28**, 581–600 (1996).
- [17] R. Penrose, “On the Gravitization of Quantum Mechanics 1: Quantum State Reduction,” *Foundations of Physics* **44**, 557–575 (2014).
- [18] T. Jacobson, “Thermodynamics of spacetime: the Einstein equation of state,” *Physical Review Letters* **75**, 1260 (1995).
- [19] D. N. Page and C. D. Geilker, “Indirect Evidence for Quantum Gravity,” *Phys. Rev. Lett.* **47**, 979–982 (1981).
- [20] C. J. Isham, “Canonical quantum gravity and the problem of time,” in *Integrable systems, quantum groups, and quantum field theories*, pp. 157–287. Springer, 1993.
- [21] K. Eppley and E. Hannah, “The necessity of quantizing the gravitational field,” *Foundations of Physics* **7**, 51 (1977).
- [22] C. Marletto and V. Vedral, “Why we need to quantise everything, including gravity,” *NPJ Quantum Information* **3**, (2017).
- [23] C. Kiefer, “Quantum Gravity,” in *Springer Handbook of Spacetime*, A. Ashtekar and V. Petkov, eds., pp. 709–722. 2014.
- [24] C. Marletto and V. Vedral, “Witness gravity’s quantum side in the lab,” *Nature* **547**, 156–158 (2017).
- [25] C. Marletto and V. Vedral, “Gravitationally Induced Entanglement between Two Massive Particles is Sufficient Evidence of Quantum Effects in Gravity,” *Phys. Rev. Lett.* **119**, 240402 (2017).
- [26] S. Bose, A. Mazumdar, G. W. Morley, H. Ulbricht, M. Toroš, M. Paternostro, A. A. Geraci, P. F. Barker, M. S. Kim, and G. Milburn, “Spin Entanglement Witness for Quantum Gravity,” *Phys. Rev. Lett.* **119**, 240401 (2017).
- [27] D. Kafri and J. M. Taylor, “A noise inequality for classical forces,” *ArXiv e-prints* (2013), [arXiv:1311.4558](https://arxiv.org/abs/1311.4558) [quant-ph].
- [28] N. Altamirano, P. Corona-Ugalde, R. B. Mann, and M. Zych, “Unitarity, feedback, interactionsdynamics emergent from repeated measurements,” *New Journal of Physics* **19**, 013035 (2017).
- [29] H. M. Wiseman and G. J. Milburn, *Quantum Measurement and Control*. Cambridge University Press, Cambridge, 2010.
- [30] K. Jacobs, *Quantum measurement theory and its applications*. Cambridge University Press, 2014.
- [31] R. Colella, A. W. Overhauser, and S. A. Werner, “Observation of gravitationally induced quantum interference,” *Physical Review Letters* **34**, 1472 (1975).
- [32] V. V. Nesvizhevsky, H. G. Börner, A. K. Petukhov, H. Abele, S. Baeßler, F. J. Rueß, T. Stöferle, A. Westphal, A. M. Gagarski, G. A. Petrov, et al., “Quantum states of neutrons in the Earth’s gravitational field,” *Nature* **415**, 297–299 (2002).
- [33] G. Rosi, F. Sorrentino, L. Cacciapuoti, M. Prevedelli, and G. Tino, “Precision measurement of the Newtonian gravitational constant using cold atoms,” *Nature* **510**, 518–521 (2014).
- [34] G. Rosi, L. Cacciapuoti, F. Sorrentino, M. Menchetti, M. Prevedelli, and G. M. Tino, “Measurement of the Gravity-Field Curvature by Atom Interferometry,” *Phys. Rev. Lett.* **114**, 013001 (2015).
- [35] P. Asenbaum, C. Overstreet, T. Kovachy, D. D. Brown, J. M. Hogan, and M. A. Kasevich, “Phase Shift in an Atom Interferometer due to Spacetime Curvature across its Wave Function,” *Phys. Rev. Lett.* **118**, 183602 (2017).
- [36] D. Kafri, J. M. Taylor, and G. J. Milburn, “A classical channel model for gravitational decoherence,” *New J. Phys.* **16**, 065020 (2014).
- [37] D. Kafri, G. J. Milburn, and J. M. Taylor, “Bounds on quantum communication via Newtonian gravity,” *New J. Phys.* **17**, 015006 (2015).
- [38] T. Kovachy, P. Asenbaum, C. Overstreet, C. Donnelly, S. Dickerson, A. Sugarbaker, J. Hogan, and M. Kasevich, “Quantum superposition at the half-metre scale,” *Nature* **528**, 530–533 (2015).
- [39] A. Sugarbaker, “Atom interferometry in a 10 m fountain, Stanford, 2014.”
- [40] A. Bassi, K. Lochan, S. Satin, T. P. Singh, and H. Ulbricht, “Models of Wave-function Collapse, Underlying Theories, and Experimental Tests,” *Rev. Mod. Phys.* **85**, 471–527 (2013).
- [41] M. A. Nielsen and I. L. Chuang, *Quantum Computation and Quantum Information*. Cambridge, 2000.
- [42] D. Stamper-Kurn, G. Marti, and H. Müller, “Verifying quantum superpositions at metre scales,” *Nature* **537**, E1 (2016).
- [43] S. Eibenberger, S. Gerlich, M. Arndt, M. Mayor, and J. Tüxen, “Matter–wave interference of particles selected from a molecular library with masses exceeding 10000 amu,” *Physical Chemistry Chemical Physics* **15**, 14696–14700 (2013).
- [44] M. Sclafani, T. Juffmann, C. Knobloch, and M. Arndt, “Quantum coherent propagation of complex molecules through the frustule of the alga *Amphipleura pellucida*,” *New Journal of Physics* **15**, 083004 (2013).
- [45] I. Pikovski, “On Quantum Superpositions in an Optomechanical System,” diploma thesis, Freie Universität

- Berlin, 2009.
- [46] I. Dutta, D. Savoie, B. Fang, B. Venon, C. L. Garrido Alzar, R. Geiger, and A. Landragin, “Continuous Cold-Atom Inertial Sensor with 1 nrad/sec Rotation Stability,” *Phys. Rev. Lett.* **116**, 183003 (2016).
- [47] R. Schnabel, “Einstein-Podolsky-Rosen-entangled motion of two massive objects,” *Phys. Rev. A* **92**, 012126 (2015).
- [48] T. Quinn, H. Parks, C. Speake, and R. Davis, “Improved Determination of G Using Two Methods,” *Phys. Rev. Lett.* **111**, 101102 (2013).
- [49] P. J. Mohr, D. B. Newell, and B. N. Taylor, “CODATA recommended values of the fundamental physical constants: 2014*,” *Rev. Mod. Phys.* **88**, 035009 (2016).
- [50] N. Altamirano, P. Corona-Ugalde, K. E. Khosla, G. J. Milburn, and R. B. Mann, “Emergent dark energy via decoherence in quantum interactions,” *Classical and Quantum Gravity* **34**, 115007 (2017).
- [51] K. E. Khosla and N. Altamirano, “Detecting gravitational decoherence with clocks: Limits on temporal resolution from a classical-channel model of gravity,” *Physical Review A* **95**, 052116 (2017).
- [52] R. Pascale, N. Altamirano, and R. B. Mann, “Emergent Dark Energy in Classical Channel Gravity with Matter,” *ArXiv e-prints* (2017), [arXiv:1706.02312 \[gr-qc\]](https://arxiv.org/abs/1706.02312).
- [53] G. C. Ghirardi, P. Pearle, and A. Rimini, “Markov processes in Hilbert space and continuous spontaneous localization of systems of identical particles,” *Phys. Rev. A* **42**, 78–89 (1990).
- [54] D. Giulini and A. Großardt, “Gravitationally induced inhibitions of dispersion according to a modified Schrödinger–Newton equation for a homogeneous-sphere potential,” *Classical and Quantum Gravity* **30**, 155018 (2013).
- [55] M. J. W. Hall and M. Reginatto, “On two recent proposals for witnessing nonclassical gravity,” *Journal of Physics A: Mathematical and Theoretical* **51**, 085303 (2018).
- [56] C. M. Caves and G. J. Milburn, “Quantum-mechanical model for continuous position measurements,” *Phys. Rev. A* **36**, 5543–5555 (1987).

Appendix A: Essentials of Classical Channel Gravity

We describe here the basic features of Classical Channel Gravity as originally discussed by KTM [36]. The key premise is that Newtonian gravity is a fundamentally classical interaction that cannot increase entanglement between any two systems. This premise is applicable to any non-relativistic system, though the original proposal considered a pair of harmonic oscillators for testing that idea.

This can most easily be derived in the context of collisional dynamics. A collisional model with a time-scale τ describes evolution of the state as $\rho_s(t + \tau) = \text{Tr}_A\{\hat{U}(\tau)(\rho_s \otimes \rho_a)\hat{U}^\dagger(\tau)\}$, where ρ_s and ρ_a are the density matrices of the system and the environment (ancillae), respectively, and $\hat{U}(\tau)$ describes their joint unitary evolution; the trace is over the ancillae.

The original KTM model as defined in ref. [36] considers a quasi one-dimensional setting of two essentially point-like massive particles. At each step of the collisional dynamics the massive particles interact with ancillas a_1, a_2 via two interaction terms: the “measurement” interaction: $\hat{x}_1 \otimes \hat{p}_{a_1} + \hat{x}_2 \otimes \hat{p}_{a_2}$ (where ancilla obtain information about the positions of the particles) and the “feedback” interaction $K\hat{x}_1 \otimes \hat{x}_{a_2} + K\hat{x}_2 \otimes \hat{x}_{a_1}$ (where ancilla induce a force on the particles depending on the information about the position of the other mass, acquired in the “measurement” step). Here \hat{x}_i , $i = 1, 2$ are the position operators of the i^{th} mass, and $\hat{x}_{a_j}, \hat{p}_{a_j}$, $j = 1, 2$ are position and momentum operators of the j^{th} ancilla. For the state of ancillas giving rise to finite effective dynamics (e.g Gaussian states with width σ) and in the continuous-interaction limit of $\tau \rightarrow 0$ the following master equation results [28–30, 56]:

$$\dot{\rho}_s = -\frac{i}{\hbar}[\hat{H}_0 + K\hat{x}_1\hat{x}_2, \rho_s] - \left(\frac{1}{4D} + \frac{K^2 D}{4\hbar^2}\right) \sum_{i=1,2} [\hat{x}_i, [\hat{x}_i, \rho_s]],$$

where $D := \lim_{\tau \rightarrow 0, \sigma \rightarrow \infty} \tau\sigma$ – this corresponds to a limit in which increasingly imprecise measurement of broad width σ occur with increasing rapidity τ such that the product $\tau\sigma$ remains finite [28]. The form of the “measurement” and “feedback” terms is fixed by the assumptions of local system–ancilla interactions and the desired form of the effective system–system interaction, up to the rescaling by α and $1/\alpha$ of the “measurement” and “feedback” interactions, respectively. Such a reparametrisation, however, returns the same model, i.e. with the same minimal bound on the decoherence rate. We note that ref. [36] studied a special case with $K := 2\frac{Gm_1m_2}{d^3}$ and \hat{H}_0 describing two harmonic oscillators with masses m_1, m_2 , where the effective unitary term $K\hat{x}_1\hat{x}_2$ could be interpreted as the normal mode splitting due to an effective Newtonian potential.

By adding to the “feedback” interaction local terms $-\frac{d^2 K}{2} \left(\frac{1}{2} + \frac{\hat{x}_1 + \hat{x}_2}{d} + \frac{\hat{x}_1^2 + \hat{x}_2^2}{d^2}\right)$ acting trivially on the ancilla, the effective unitary term becomes

$$V_0 = -G\frac{m_1m_2}{d} \left(1 - \frac{x_1 + x_2}{d} + \left(\frac{x_1 + x_2}{d}\right)^2\right)$$

which approximates Newtonian gravitational potential $-G\frac{m_1m_2}{|X_1 - X_2|}$ up to second order in x_1, x_2 ; $X_1 - X_2 \equiv d + x_1 + x_2$. This

extension recovers the homogeneous part of the potential in addition to the force gradients and yields

$$\dot{\rho}_s = -\frac{i}{\hbar}[\hat{H}_0 + V_0, \rho_s] - \left(\frac{1}{4D} + \frac{K^2 D}{4\hbar^2} \right) \sum_{i=1}^2 [\hat{x}_i, [\hat{x}_i, \rho_s]]. \quad (\text{A1})$$

which is the main-text eq. (1). It can be applied with any H_0 , e.g. that of two free particles with masses m_1, m_2 . In such a case the overall unitary term (first commutator) describes the standard dynamics of two massive particles interacting via Newtonian potential, while the non-unitary terms ensure that the resulting channel is entanglement non increasing.

We emphasize that there is no requirement that the two massive systems are in any specific state, such as Gaussian states. However, specific states can be employed to provide an independent argument for a lower bound on decoherence in the KTM approach: the KTM lower bound coincides with the lower bound that guarantees that entanglement specifically between Gaussian states does not increase [36]. The key feature of the dynamics described in eq. (A1) – that it is entanglement non-increasing – is independent of how it is derived: from a classical stochastic model of the environment (ancillae) [29] or from a quantum collisional model [28]. It is a generic feature of LOCC channels (realized via local interactions and communication of classical information) that they cannot increase entanglement.

Appendix B: KTM model for composite systems

Here we extend the KTM approach by constructing a model for composite systems in three dimensions relevant for the matter wave experiments we analyze in the main text. We consider two systems s_1 and s_2 respectively consisting of N_1 and N_2 elementary constituents – chosen to be atoms – with masses m_i , $i = 1, \dots, N_1 + N_2$. Choosing atoms to be the basic constituents of a body ensures that (unlike the case for subatomic particles) the total mass of a body is equal to the sum of its individual constituents. Our aim is to describe the behaviour of the centres of mass of two objects in the KTM model, thereby allowing a more complete comparison between it and the Diosi-Penrose model. A multi-particle extension of the KTM model could also be used directly (though perhaps more clumsily) and the same final results would be obtained.

The classical gravitational potential energy between any two constituents i, j reads

$$V_{ij} = \frac{Gm_i m_j}{|\vec{r}_{ij}|},$$

where \vec{r}_{ij} is the vector joining the positions of the individual masses m_i, m_j . We write this as $\vec{r}_{ij} = \vec{d}_{ij} + \vec{x}_i + \vec{x}_j$, where \vec{d}_{ij} is the vector joining their positions at the initial time and $\vec{x}_{i,j}$ is the displacement of the CM of a given body. We consider the case where s_1 and s_2 are rigid. In applications of interest here, s_1 will be a test mass (e.g. an atom in an interferometer) and s_2 will describe matter gravitationally interacting with s_1 , (e.g. the Earth). We will thus assume that a) all constituents of a given body are in a superposition of equally distant locations (rigidity); b) there is one distinguished direction defined by the superposition of the test mass (while the surrounding matter is well localised), see fig. 2.

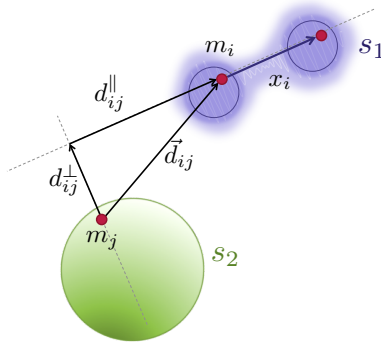


FIG. 2. Test body s_1 in a spatial superposition in the presence of a source mass s_2 . For any pair of elementary masses (m_i, m_j) forming the bodies, the distance \vec{d}_{ij} between them can be decomposed into component d_{ij}^{\parallel} along the direction of the spatial superposition of s_1 and a perpendicular component d_{ij}^{\perp} . x_i is the displacement from the initial position of the mass m_i , whose values span all locations between which the particle can be superposed. Note that the assumption of rigidity implies that each constituent of s_1 is displaced by the same amount.

It is convenient to write $\vec{d}_{ij} = d_{ij}^{\parallel} \hat{e} + d_{ij}^{\perp} \hat{e}^{\perp}$ where $\vec{x}_i = x_i \hat{e}$ and thus \hat{e} is a unit vector in the direction defined by the

superposition and \hat{e}^\perp is a unit vector in an orthogonal direction. With the above we can write

$$V_{ij} = \frac{-Gm_i m_j}{\sqrt{(d_{ij}^\parallel + x_i + x_j)^2 + (d_{ij}^\perp)^2}} \approx -Gm_i m_j \times \left(\frac{1}{d_{ij}} - \frac{d_{ij}^\parallel}{d_{ij}^3}(x_i + x_j) + \frac{(d_{ij}^\parallel)^2 - \frac{1}{2}(d_{ij}^\perp)^2}{d_{ij}^5}(x_i + x_j)^2 \right) \quad (\text{B1})$$

where $d_{ij} = \sqrt{(d_{ij}^\parallel)^2 + (d_{ij}^\perp)^2}$.

For any pair (i, j) the “measurement” part of the interaction can thus be taken as $\hat{x}_i \otimes \hat{p}_{m_i} + \hat{x}_j \otimes \hat{p}_{m_j}$ and the “feedback” as $K_{ij}\hat{x}_i \otimes \hat{x}_{m_j} + K_{ij}\hat{x}_j \otimes \hat{x}_{m_i} + \hat{Y}_i \otimes \hat{I}_{m_j} + \hat{Y}_j \otimes \hat{I}_{m_i}$, where $\hat{Y}_{i(j)}$ acts only on mass $m_{i(j)}$. The following master equation for the pair

$$\dot{\rho}_{ij} \approx -\frac{i}{\hbar}[\hat{H}_0 + \hat{Y}_i + \hat{Y}_j + K_{ij}\hat{x}_i\hat{x}_j, \rho_{ij}] - \Gamma_{ij}([\hat{x}_i, [\hat{x}_i, \rho_{ij}]] + [\hat{x}_j, [\hat{x}_j, \rho_{ij}]])$$

is thus obtained, where $\Gamma_{ij} \equiv \frac{1}{4D} + \frac{K_{ij}^2 D}{4\hbar^2}$. Defining $K_{ij} := 2Gm_i m_j \frac{(d_{ij}^\parallel)^2 - \frac{1}{2}(d_{ij}^\perp)^2}{d_{ij}^5}$, $Y_i := -Gm_i m_j (\frac{1}{2d_{ij}} - \frac{d_{ij}^\parallel}{d_{ij}^3}x_i + \frac{(d_{ij}^\parallel)^2 - \frac{1}{2}(d_{ij}^\perp)^2}{d_{ij}^5}x_i^2)$ the master equation describes the induced (approximate) Newtonian interaction between m_i, m_j (since $\hat{Y}_i + \hat{Y}_j + K_{ij}\hat{x}_i\hat{x}_j \approx V_{ij}$, eq. (B1)) with the decoherence term including a gradient of the Newtonian force between the pair, as in the eq. (A1) but in three dimensions. Note that the x -axis is defined by the direction of the superposition; that is why decoherence terms included in the model also act only in this direction. The dynamics of all $N_1 + N_2$ constituents, described by ρ_{tot} , reads

$$\dot{\rho}_{tot} = -\frac{i}{\hbar}[\hat{H}_0 + \sum_{i < j}^{N_1+N_2} V_{ij}, \rho_{tot}] - \sum_{i < j}^{N_1+N_2} \Gamma_{ij}([\hat{x}_i, [\hat{x}_i, \rho_{tot}]] + [\hat{x}_j, [\hat{x}_j, \rho_{tot}]]) \quad (\text{B2})$$

Introducing the displacement r_1 (r_2) of the CM of s_1 (s_2), and \hat{x}'_i as the displacement relative to the CM, the displacement of any individual constituent can be described by $\hat{x}_i = \hat{r}_1 + \hat{x}'_i$ for $i < N_1$ (for constituents of s_1) and $\hat{x}_i = \hat{r}_2 + \hat{x}'_i$ for $i > N_1$ (for constituents of s_2). With the above $[\hat{x}_i, [\hat{x}_i, \rho_{tot}]] = [\hat{r}_1, [\hat{r}_1, \rho_{tot}]] + [\hat{x}'_i, [\hat{x}'_i, \rho_{tot}]] + [\hat{r}_1, [\hat{x}'_i, \rho_{tot}]] + [\hat{x}'_i, [\hat{r}_1, \rho_{tot}]]$, for $i \leq N_1$ and analogously (with \hat{r}_2 instead of \hat{r}_1) for $i > N_1$. From the assumed rigidity of the bodies it follows that relative degrees of freedom are uncorrelated with the CM and their displacements remain negligible; see fig. 3 for an illustration (i.e. a rigid body whose CM is in a superposition of locations a and b is described by a correlated state where all its constituents are at fixed distances relative to the CM position a and at the same fixed distances relative to the CM position b).

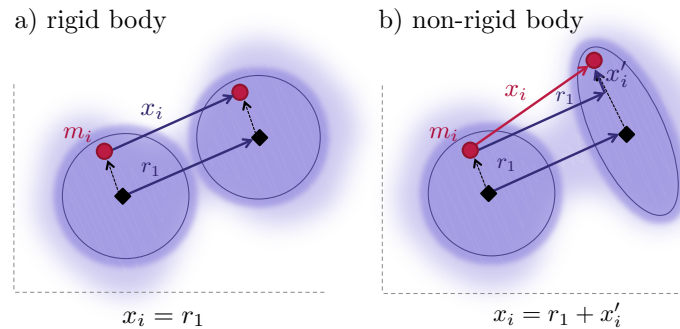


FIG. 3. Displacement x_i of the i^{th} constituent of a) rigid body, b) non-rigid body. For a rigid body each constituent remains at the same distance (dashed arrow) from the centre mass (black diamond), and its displacement is the same as that of CM $x_i = r_1$. For a non-rigid body, the displacement of a constituent can differ from that of the centre of mass, $x_i = r_1 + x'_i$. This work only considers case a).

Tracing over the relative degrees of freedom and keeping the CM positions of s_1 and s_2 results in the following master equation (in performing the trace, for simplicity one can assume that the CM of s_i coincides with the position of one of its

particles)

$$\begin{aligned} \dot{\rho}_{s_1 s_2} = & -\frac{i}{\hbar} [\hat{H}_0 + V, \rho_{s_1 s_2}] - 2 \sum_{i < j=1}^{N_1} \Gamma_{ij} [\hat{r}_1, [\hat{r}_1, \rho_{s_1 s_2}]] - 2 \sum_{N_1 < i < j}^{N_1+N_2} \Gamma_{ij} [\hat{r}_2, [\hat{r}_2, \rho_{s_1 s_2}]] \\ & - \sum_{i=1}^{N_1} \sum_{j=N_1+1}^{N_1+N_2} \Gamma_{ij} \left([\hat{r}_1, [\hat{r}_1, \rho_{s_1 s_2}]] + [\hat{r}_2, [\hat{r}_2, \rho_{s_1 s_2}]] \right) \end{aligned} \quad (\text{B3})$$

where $V = \sum_{i < j}^{N_1+N_2} V_{ij} \approx -G \frac{M_1 M_2}{[d+r_1+r_2]}$; M_1 and M_2 are correspondingly the total masses of s_1 and s_2 .

Finally, tracing over the degrees of freedom of s_2 one obtains the master equation for the CM of s_1 :

$$\dot{\rho}_{s_1} = -\frac{i}{\hbar} [\hat{H}_0 + V, \rho_{s_1}] - \left(2 \sum_{i < j=1}^{N_1} \Gamma_{ij} + \sum_{i=1}^{N_1} \sum_{j=N_1+1}^{N_1+N_2} \Gamma_{ij} \right) [\hat{r}_1, [\hat{r}_1, \rho_{s_1}]], \quad (\text{B4})$$

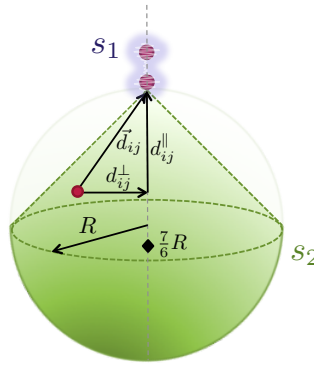


FIG. 4. Estimation of the decoherence effect on a single atom, s_1 , due to Earth: for simplicity we consider only the portion of Earth for which the decoherence rate is always greater than the effect stemming from matter concentrated at its centre of mass. This portion of Earth's mass is defined as all constituents (atoms) for which $d_{1j}^\perp < d_{1j}^\parallel$ – inside the cone-and-half-ball, shaded green in the figure. The total mass of the region is $3/4$ of the mass of Earth M , and its centre of mass is $7/6$ of the Earth's radius R .

We are particularly interested in the case when s_1 is a single atom, $N_1 = 1$, and s_2 is the entire Earth. Minimising the decoherence rate for each pair $(1, j)$ gives $\Gamma_{1j}^{min} = \frac{K_{1j}}{2\hbar}$ and the total decoherence rate is given by $\sum_{j \in \text{earth}} \frac{K_{1j}}{2\hbar}$. Note, that every constituent of the Earth acts so as to increase the decoherence rate of s_1 . Here we seek to relate the resulting decoherence to that given by the Earth's CM, as in the original model. (For some geometries, the multi-particle formulation of the model, and the original KTM prediction for the CMs of the bodies give different results¹.) Since K_{1j} as a function of $(d_{1j}^\parallel, d_{1j}^\perp)$ is convex only for $|d_{1j}^\parallel| < |d_{1j}^\perp|/\sqrt{2}$ we consider only a portion \mathcal{C} of the Earth's mass, which lies within the volume where K_{1j} is convex, see fig. 4.

The overall decoherence rate is greater than that stemming from particles in \mathcal{C} , which itself is greater than decoherence coming from the centre of mass of \mathcal{C} . Since $|d_{1j}^\parallel| < |d_{1j}^\perp|/\sqrt{2} < |d_{1j}^\perp|$, the region \mathcal{C} can be taken as a cone of height R and support of area πR^2 together with a half ball of radius R . Assuming a constant density for body M_2 , the mass of \mathcal{C} is $\frac{3}{4}M_2$ and its CM is at a distance $\frac{7}{6}R$ from the top surface, as depicted in fig. 4. The quantity

$$\Gamma_{M_2;R}^{min} = \frac{3}{4} \left(\frac{6}{7} \right)^3 \Gamma_{KTM}(M_1, M_2, R) = 0.47 \Gamma_{KTM}(M_1, M_2, R)$$

¹ Let s_2 to be a spherical shell of radius r comprising N particles of mass m , and s_1 – an elementary particle inside the shell. Sum over the constituents of the shell yields a finite decoherence rate, which can be made arbitrar-

ily small by increasing $r \rightarrow \infty$. However, decoherence predicted by the model applied directly to the CM of s_2 is arbitrarily large for s_1 arbitrarily close to the shell's centre, independently of r .

where $\Gamma_{KTM}(M_1, M_2, R) = \frac{GM_1M_2}{R^3}$ is the lower bound on the decoherence rate of mass M_1 due to the presence of the homogeneous ball of mass M_2 and radius R . Note that in the above the $\Gamma_{KTM}(M_1, M_2, R)$ is the decoherence rate as per the original KTM model for elementary masses M_1, M_2 at a distance R .

Note that our overall result is lower bounded by the decoherence rate calculated as if the entire body were concentrated in the centre of mass. Hence the predictions of the KTM model for the experiments we analyze will not change if we choose constituents of the Earth that are different from atoms.

We close this section by noting that in general there will be decoherence also in the transverse directions. However the setup we analyze is not sensitive to any loss of coherence in transverse directions. Furthermore, any such effects will further increase decoherence rates, and thus will not affect our results.

Appendix C: Torsion Balance

Here we consider an application of the KTM approach to torsion balance experiments. These experiments measure the gravitational constant G by balancing the torque produced by the gravitational attraction between massive objects situated on the balance. We show here how the measurement/feedback model can be used to simulate a classical potential in this context.

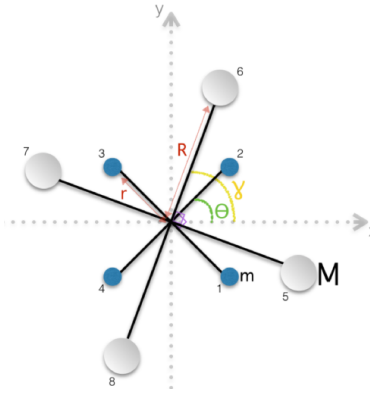


FIG. 5. Set-up of the torsion balance experiment.

The Hamiltonian of the system is

$$H = \sum_i \frac{1}{2} m_i (\dot{x}_i^2 + \dot{y}_i^2) + \sum_{i,j} V_{ij}, \quad (C1)$$

where i runs over all (spherical) bodies in the experiment and V_{ij} denotes the (Newtonian) gravitational potential between pairs of bodies, with each body regarded as a point-like object located at its centre-of-mass.

The actual experiment consists of 8 bodies, 4 identical small bodies each of mass m , and 4 other identical large bodies each of mass M , as illustrated in figure 5. Since all bodies in the experiment are in the same plane, we can write the above hamiltonian as

$$\begin{aligned} H &= 2m \left(\dot{r}^2 + r^2 \dot{\theta}^2 \right) + 2M \left(\dot{R}^2 + R^2 \dot{\gamma}^2 \right) + \sum_{i,j} V_{ij} \\ &= 2mr^2 \dot{\theta}^2 + 2MR^2 \dot{\gamma}^2 + \sum_{i < j} V_{ij} \end{aligned} \quad (C2)$$

in polar coordinates (r, θ) and (R, γ) for the small and large bodies respectively, where the latter relation follows from the rigidity of the balance arms. The setup of the experiment ensures that V_{ij} depends only on the variable $\alpha = \gamma - \theta$, and so

$$\begin{aligned} H &= \frac{mr^2 + MR^2}{4mr^2MR^2} p_\alpha^2 + \frac{p_\xi^2}{4(mr^2 + MR^2)} + \frac{4GmM}{\sqrt{r^2 + R^2 + 2rR \cos \alpha}} + \frac{4GmM}{\sqrt{r^2 + R^2 + 2rR \sin \alpha}} \\ &\quad + \frac{4GmM}{\sqrt{r^2 + R^2 - 2rR \cos \alpha}} + \frac{4GmM}{\sqrt{r^2 + R^2 - 2rR \sin \alpha}} + \frac{4Gm^2}{\sqrt{2}r} + \frac{4GM^2}{\sqrt{2}R} + \frac{Gm^2}{r} + \frac{GM^2}{R} \end{aligned} \quad (C3)$$

where p_α is the conjugate momentum to α and p_ξ is the conjugate momentum to the variable $\xi \equiv \frac{mr^2\theta + MR^2\gamma}{mr^2 + MR^2}$.

The relevant variable is small deviations of the angle α away from its equilibrium value α_0 . Writing $\alpha = \alpha_0 + \delta\alpha$, where $\delta\alpha \ll \alpha_0$, the Hamiltonian can be approximated as

$$H = \frac{p_\alpha^2}{2I_{eff}} + \frac{p_\xi^2}{4(mr^2 + MR^2)} + B\delta\alpha + C(\delta\alpha)^2 + \dots \quad (C4)$$

where $I_{eff} = \frac{2mr^2MR^2}{mr^2 + MR^2}$ is the reduced moment of inertia and

$$B = \sum_{n=1}^3 \frac{4GmMrR \sin(\alpha_0 + (n+1)\pi/2)}{(r^2 + R^2 - 2rR \sin(\alpha_0 + n\pi/2))^{\frac{3}{2}}}$$

$$C = -\sum_{n=1}^3 \frac{2GmMrR \sin(\alpha_0 + n\pi/2)}{(r^2 + R^2 - 2rR \sin(\alpha_0 + n\pi/2))^{\frac{3}{2}}} + \sum_{n=1}^3 \frac{6GmMr^2R^2 \sin^2(\alpha_0 + (n+1)\pi/2)}{(r^2 + R^2 - 2rR \sin(\alpha_0 + n\pi/2))^{\frac{5}{2}}} \quad (C5)$$

and we have dropped the irrelevant constant terms from (C3).

In the context of the general master equation (A1), we have $\hat{x} \rightarrow \delta\hat{\alpha} \equiv \Delta\alpha$, and $K = 2C$. Writing $D = \frac{\hbar}{2C\epsilon}$, we obtain

$$\dot{\rho} = -\frac{i}{\hbar} \left[\frac{\hat{p}_\alpha^2}{2I_{eff}} + \frac{\hat{p}_\xi^2}{4(mr^2 + MR^2)} + B\delta\hat{\alpha} + C\delta\hat{\alpha}^2, \rho \right] - \frac{C}{2\hbar} \left(\epsilon + \frac{1}{\epsilon} \right) [\delta\hat{\alpha}, [\delta\hat{\alpha}, \rho]] \quad (C6)$$

To empirically constrain the KTM model using this class of experiments, we adopt the perspective that world measurements on Newton's constant G [49] have a certain degree of scatter, and that this scatter can provide a bound on how large the gravitational repeated-measurement-feedback effect from (C6) is. We have assumed that the bodies are pointlike, but as we have seen from earlier sections taking into account the finite size of the bodies will lead to corrections in D (or Γ) that are of order unity.

For the Cavendish experiment the total error in G is

$$\frac{\Delta G}{G} = \frac{\delta(\Delta\alpha)}{\Delta\alpha} + \frac{\delta k}{k} - \left(\frac{\delta M}{M} + \frac{\delta m}{m} + 4\frac{\delta r_a}{r_a} + 4\frac{\delta r_b}{r_b} - 5\frac{\delta R_{ac}}{R_{ac}} - 5\frac{\delta R_b}{R_b} + \alpha_{CT} \right) + \frac{\delta\tau_c}{\tau_c} \quad (C7)$$

where the meaning of these various quantities is explained in Ref. [48] (see equation (11.10) therein). The minimal constraint on $\Delta\alpha$ is therefore

$$\left| \frac{\delta(\Delta\alpha)}{\Delta\alpha} \right| \leq \left| \frac{\Delta G}{G} \right|$$

where $\Delta\alpha = |\langle(\delta\hat{\alpha})^2\rangle|$ and $\delta(\Delta\alpha) = \sqrt{\langle(\delta\hat{\alpha})^2\rangle}$, the latter quantity being the time-averaged variance computed from the repeated measurement process. This quantity is

$$\langle(\delta\hat{\alpha})^2\rangle = \frac{\hbar}{8I_{eff}} T \left(\epsilon + \frac{1}{\epsilon} \right)$$

where T is the timescale over which the experiment is performed.

To estimate the size of $\delta(\Delta\alpha)$, we have $m = 1.2$ kg, $M = 11$ kg, $r = 120$ mm, $R = 214$ mm, and $\alpha_0 = 18.9^\circ$, yielding $I_{eff} = 8.35 \times 10^{-3}$ kg m². Hence

$$\langle(\delta\hat{\alpha})^2\rangle = 1.58 \times 10^{-33} T \left(\epsilon + \frac{1}{\epsilon} \right) \text{ s}^{-1}$$

Consequently

$$\left| \frac{\delta(\Delta\alpha)}{\Delta\alpha} \right| = \sqrt{1.58 \times 10^{-33} T \left(\epsilon + \frac{1}{\epsilon} \right)} \leq \left| \frac{\Delta G}{G} \right| \sim 10^{-6}$$

$$\Rightarrow T \left(\epsilon + \frac{1}{\epsilon} \right) \leq \sim 6 \times 10^{20} \quad (C8)$$

for $\Delta\alpha \sim 1$ radian. For an experiment on the order of 1 day = 3600 × 24 = 86400 seconds, then

$$\left(\epsilon + \frac{1}{\epsilon} \right) \leq \sim 7 \times 10^{15}$$

and the decoherence rate satisfies

$$\frac{C}{2\hbar}(\epsilon + \frac{1}{\epsilon}) \leq \sim 3.7 \times 10^{40}.$$

A more sophisticated treatment involving the compositeness of the bodies in the torsion balance will provide corrections of order unity to C . Since the above constraint is much weaker than that provided by the fountain experiments we shall not pursue this any further.